UCRL 15318

MASTER

An Evaluation of 2¼ Cr—1 Mo Steel for Liquid Lithium Containment

II. Effects of Post-Weld Heat Treatment and Niobium Content

Annual Report
1979

T.L. Anderson
G.R. Edwards

Department of Metallurgical Engineering
Colorado School of Mines
Golden, Colorado 80401

Prepared for
Lawrence Livermore Laboratories
Under Purchase Order No. 8818503

TABLE OF CONTENTS

INTRODUCTION

Previous Lithium Corrosion Studies

Liquid lithium corrosion of pure metals and alloys was initially studied by a number of investigators[1-6] to obtain relative corrosion resistance data for material selection. Failure to recognize the importance of impurity contamination and dissimilar-metal mass transfer effects resulted in a great deal of scatter and contradiction in the results.

The principal factors affecting the severity of corrosion attack have been found to be temperature, temperature gradient, cyclic temperature fluctuation, ratio of material area to lithium volume, impurity level in the lithium, flow velocity, the material's surface condition, the number of solid materials in contact with the lithium, and the metallurgical condition of the container material. Roughly speaking, these factors are listed in order of decreasing importance. More complete discussions of these mechanisms and controlling factors may be found in other references[1,6-9].

Summarizing these results for a large number of alloys, it has been found that:

1. Pure iron has good corrosion resistance to lithium up to approximately 1000C[1,10,11]. Iron is subject to intergranular attack if carbon and/or nitrogen are present in either the lithium or the iron[1]. The rate of attack is greatly increased if the iron is stressed[10,12]. The corrosion resistance decreases with

increasing carbon content because Fe_3C can be reduced to form Li_2C_2, which may cause internal stresses and cracking because of its lower density[13]. In general, any steel having significant amounts of Fe_3C will have unsatisfactory corrosion resistance. Very little research has been performed evaluating the lithium corrosion resistance of steels. Beskorovainyi, et al.[14] performed preliminary evaluations on plain carbon steel, and Selle[15] presented data which indicated that 2 1/4 Cr - 1 Mo steel was resistant to lithium corrosion when the nitrogen concentrations in the lithium were low.

2. Stainless steels are more attractive than iron because of their increased strength, but their corrosion resistance is not as good. Austenitic stainless steels are limited to approximately 500C in dynamic, long-time applications[16]. Austenitic stainless is subject to preferential dissolution of nickel and chromium, resulting in a ferritic surface layer[1,3,17-19]; the severity of leaching increases with increasing nickel or chromium content[20]. The presence of nitrogen and/or carbon is also known to increase the rate of nickel and chromium mass transfer[8,21,22] as well as to give rise to severe grain boundary attack[23-25]. Carbon in lithium has been reported to result in carburization of chromium steels[13], whereas carbon in the steel itself results in chromium carbide formation; the resultant chromium-depleted zone may then be subject to nickel

leaching[26]. A similar effect has been observed in the depleted zone around sigma phase particles[26,27]. Ferritic stainless steels have better corrosion resistance than austenitic steels, but are still subject to chromium leaching. The low carbon, low chromium steels have been reported to be superior to steels with higher chromium and carbon[4,20].

3. Nickel- and cobalt-base alloys have been reported to have poor corrosion resistance in lithium. In static, isothermal tests, they have experienced intergranular attack[23,28,29]. In loop tests, both are subject to severe dissolution attack, probably as a result of the high solubilities of nickel and cobalt in liquid lithium[1,30].

4. The refractory metals and alloys generally have good resistance to lithium even at very high temperatures. Molybdenum and its alloys have been tested at 1650C for 1000 hours and found to give good service, even in the presence of oxygen and nitrogen contamination[4,7,31,32]. Zirconium is reported to give satisfactory performance in loops at 816C[1]. Niobium and tantalum give good service, but are subject to attack in the presence of oxygen[13,33,34]. It has been suggested that the nitrides of titanium and zirconium and the carbides of niobium and tantalum may form on the metal surface and hence act as a protective diffusion barrier[3].

Lithium Corrosion Studies for Hylife

The Hylife plant concept, wherein the first structural wall is protected by a thick liquid lithium blanket, remains an extremely viable design for controlled laser fusion. Neutron damage in the first structural wall is significantly reduced, making an evaluation of liquid lithium corrosion susceptibility one of the major alloy selection criteria.

Engineering alloys for lithium containment in the Hylife plant must meet criteria of availability, fabricability and code acceptance in addition to being acceptably resistant to liquid lithium corrosion. The major potential candidates have traditionally been 304 stainless steel and 2 1/4 Cr - 1 Mo steel (either unstabilized or Nb-stabilized). Data generated by the Colorado School of Mines under the first contract year of this program indicate that both alloys have good resistance to liquid lithium attack. However, cost and availability of 304 stainless steel make it less desirable than 2 1/4 Cr - 1 Mo steel. An additional consideration is that relatively long-lived radioactive isotopes are produced in 304 stainless steel when nickel atoms in the alloy are subjected to a high neutron flux.

The pressure vessel steel 2 1/4 Cr - 1 Mo has become the most viable candidate for lithium containment. Data generated by the Colorado School of Mines in the first contract year indicate that corrosion rates of parent metal 2 1/4 Cr - 1 Mo in high-nitrogen liquid lithium are less than those found for 304 stainless steel. However, significant grain boundary penetration in heat affected zones of GTA-welded coupons of 2 1/4 Cr - 1 Mo

was also observed. The second contract year was devoted to a systematic study of this phenomena. GTA-welded coupons of both unstabilized and Nb-stabilized 2 1/4 Cr - 1 Mo steel were given various post-weld heat treatments and subsequently exposed to low nitrogen lithium at 500C. The lithium bath contained 17.6 weight percent lead because current "heavy ion driver" fusion reactor designs utilize a lead-lithium liquid of this composition for the protective blanket. Additional corrosion tests were performed with coupons deliberately made corrosion susceptable for the purpose of gaining insights into corrosion mechanisms.

The Physical Metallurgy of 2 1/4 Cr - 1 Mo Steel

Steel of the nominal composition 2 1/4 Cr - 1 Mo has a long history of successful application in heavy structures operating at moderate temperatures. The steel is supplied under many different specifications according to application and has a complex carbide metallurgy. For that reason, a brief description of specifications and typical applications as well as a summary of the major metallurgical features should help prepare the reader for a study of the material's lithium corrosion resistance.

1. Applications and Specifications: 2 1/4 Cr - 1 Mo steel is commonly used in applications such as hydrocarbon processing plants and the steam generators of Liquid Metal Fast Breeder Reactors (LMFBR). The alloy was originally developed for service at elevated temperatures, where resistance to creep is the primary

consideration, and it is widely used for steam boiler tubes and other parts operating in the 540C to 595C (1000F to 1100F) range.

2 1/4 Cr - 1 Mo steel is currently seeing widespread use in the demanding applications of reactors and pressure vessels for new processing operations such as coal gasification and liquefaction. These applications require the increased strength, creep resistance, oxidation resistance and corrosion resistance that this alloy offers over plain carbon steels[34].

2 1/4 Cr - 1 Mo is available under ASTM specifications A213, Grade T22, for tubing; A336, Grade F22, for drum forging; A335, Grade P22, for pipe; A356, Grade 10 and A217, Grade WC9, for castings; A387, Grade D and A542, for plate. The A387D specification includes Class I (60-85 ksi tensile strength) and Class II (75-100 ksi tensile strength). The Class I heat treatment is usually an anneal, while Class II requires normalizing and tempering. The higher strength versions of 2 1/4 Cr - 1 Mo plate are covered by A542. The properties of this specification are obtained by quenching and tempering; the tensile strengths of the four classes within the A542 specification range from 85 to 125 ksi.

2. Microstructures and Heat Treatment:

a. Austenitizing: The continuous cooling transformation (CCT) diagram for 2 1/4 Cr - 1 Mo steel is shown in Figure 1[35]. Austenitizing of the alloy is usually accomplished in the 950C to 1000C temperature range. Normal commercial heat treatment practice results in one of three different conditions after austenitizing: annealed, normalized, or quenched.

The annealed structure results from slow cooling (usually furnace cooling) from the austenitizing temperature and consist of proeutectoid ferrite with typically about 20% upper bainite. The upper bainite in the annealed structure has a lamellar appearance similar to pearlite.

A somewhat faster cooling rate, on the order of 300C/hr, results in a normalized structure, which contains both proeutectoid ferrite and bainite. The resulting bainite contains both plate-like and lath-like carbides in a Widmanstatten pattern. The precipitates are mainly ε-carbide with some cementite. In addition, there is some evidence that a small amount of acicular Mo_2C exists in the normalized structure, on the ferrite side of the ferrite-bainite boundaries[36].

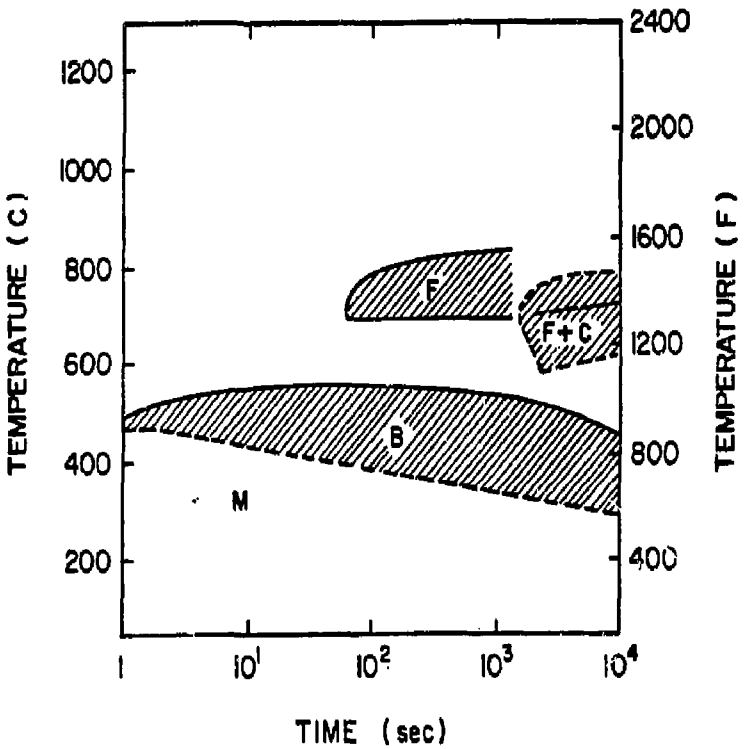

Figure 1. The continuous cooling diagram for 2¼Cr-1Mo steel.

Quenching 2 1/4 Cr - 1 Mo steel yields a microstructure of essentially 100% bainite, with the precipitates of ε-carbide in a Widmanstatten array. It is possible during quenching to obtain some minor constituents such as retained austenite, autotempered martensite or proeutectic ferrite, depending on the quenching conditions and section thickness.

As can be seen from the foregoing discussion, 2 1/4 Cr - 1 Mo steel does not possess a high degree of hardenability, as it is very difficult to form any martensite. On the other hand, unlike most other carbon and low-alloy steels, it is also very difficult to form pearlite. Therefore, the structure of 2 1/4 Cr - 1 Mo is typically a combination of proeutectoid ferrite and bainite, with the relative amounts of each being dependent on the rate of cooling from the austenitizing temperature.

Because of the relatively low hardenability of 2 1/4 Cr - 1 Mo steel, heavy sections are usually supplied in the annealed condition. In an effort to improve the hardenability of this steel (so that heavier section thicknesses could be heat treated to higher strength levels) Copeland and Pense[37] have studied the effect of varied carbon, nickel and aluminum contents on hardenability. They found that

maintaining the carbon and alloying elements at high levels suppressed the formation of low strength polygonal ferrite. They were also able to predict the strength of tempered 2 1/4 Cr - 1 Mo by knowing the ferrite content and tempering temperature.

After 2 1/4 Cr - 1 Mo steel has been austenitized and cooled to ambient temperature, the carbides present reside almost exclusively in the bainite. The ferrite contains almost no carbides and is strengthened solely by the solid solution strengthening of alloying elements.

b. Tempering: 2 1/4 Cr - 1 Mo steel can be tempered from either the quenched or normalized conditions. Tempering consists of a series of carbide precipitation and transformation reactions. These reactions have been investigated by Baker and Nutting[38] in a systematic study of the carbides present after tempering at different temperatures for various times. The carbides were evaluated using optical metallography, electron microscopy, electron diffraction, x-ray diffraction and x-ray fluorescence.

One of the significant results of this study is shown in Figure 2, where the sequence of carbide formation during tempering can be seen for both the quenched and normalized conditions. As would be expected, the precipitation reactions and kinetics

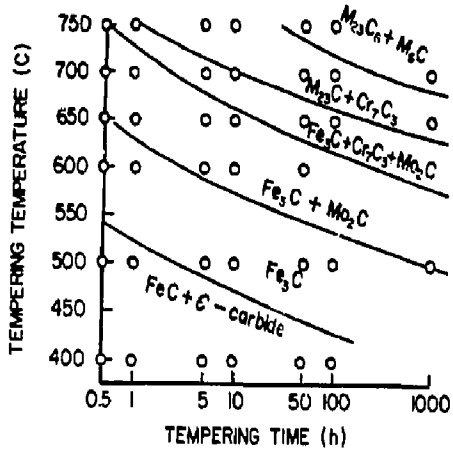

QUENCHED

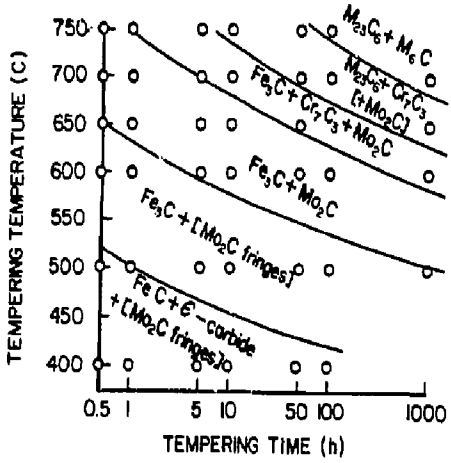

NORMALIZED

Figure 2. Carbide stability diagrams for quenched and tempered and normalized and tempered 2 1/4 Cr - 1 Mo steel.

are similar for both conditions. The difference lies in the morphology of the precipitated carbides, a consequence of different initial microstructures. As discussed previously, the as-quenched structure is totally bainite whereas the normalized structure contains a high percentage of proeutectoid ferrite. This difference shows itself mainly in the precipitation of Mo_2C. Most of the carbides formed during tempering tend to nucleate on previous carbides within the bainitic structure; however, Mo_2C nucleates within the ferrite matrix. In quenched 2 1/4 Cr - 1 Mo steel, this nucleation occurs in the ferrite within the bainite grains, whereas in normalized 2 1/4 Cr - 1 Mo steel the Mo_2C precipitates on the ferrite side of ferrite-bainite grain boundaries. This is because the bainite is the source of carbon while most of the Mo resides in the ferrite. Carbon diffusion is faster than that of molybdenum and therefore the Mo_2C precipitates tend to grow into the ferrite from the ferrite-bainite grain boundaries. Mo_2C forms somewhat more quickly in normalized steel, since it is already present to a small extent in the normalized structure.

The remainder of the carbide precipitation reactions resulting from tempering are similar for

both the quenched and normalized conditions and can be summarized in the following way:

i) Tempering quenched steel:

$$\varepsilon\text{-carbide} \rightarrow \text{cementite} \rightarrow \begin{matrix} \text{cementite} \\ + \\ Mo_2C \end{matrix} \rightarrow \begin{matrix} \rightarrow Cr_7C_3 \\ \rightarrow M_{23}C_6 \rightarrow M_6C \end{matrix}$$

ii) Tempering normalized steel:

(i) Bainite

$$\begin{matrix} \varepsilon\text{-carbide} \\ + \\ \text{cementite} \end{matrix} \rightarrow \text{cementite} \rightarrow \begin{matrix} \text{cementite} \\ + \\ Mo_2C \end{matrix} \rightarrow \begin{matrix} \rightarrow Cr_7C_3 \\ \rightarrow M_{23}C_6 \rightarrow M_6C \end{matrix}$$

(ii) Ferrite

$$Mo_2C \rightarrow M_6C$$

Epsilon carbide occurs in both normalized and quenched 2 1/4 Cr - 1 Mo and does not completely transform to cementite until after about 5 hours at 500C. As this transformation occurs, the carbide plates become thicker and the iron is partially replaced in the cementite by chromium and manganese. Upon further heating, the cementite plates begin to spherodize. Next, needle-like Mo_2C

particles nucleate and grow, as discussed previously.

Cr_7C_3 forms by nucleation either within the cementite particles or at the ferrite/cementite interface. $M_{23}C_6$ is believed[38] to nucleate at cementite boundaries where Cr_7C_3 is not already present. $M_{23}C_6$ grows at the expense of both cementite and Mo_2C, thus reducing the number of particles.

Baker and Nutting implied that all carbides eventually form M_6C (see previous diagram). Lietnaker, et al[39] found that this equilibrium carbide (called eta carbide) had a M/C ratio of approximately 4 rather than 6. The exact carbon content of this precipitate can be influenced by the chromium or oxygen content. Eta carbide may form at the expense of Mo_2C, $M_{23}C_6$, or Cr_7C_3. It is believed to be nucleated at the interfaces between existing carbides and the matrix.

3. Welding Metallurgy: In view of the complex carbide precipitation process discussed previously, problems in the welding of 2 1/4 Cr - 1 Mo steel are anticipated, particularly with high heat input welding processes (e.g. electroslag welding). As a result of the varied thermal history, a large variation in mechanical properties and microstructure from the fusion zone to

the unaffected base metal can be expected, including some temper-embrittled areas in the HAZ. To eliminate these problems, a post-weld heat treatment is usually employed. This heat treatment must be at a high enough temperature (~ 1200F) to avoid post weld stress relief embrittlement. The heat treatment tends to equalize the differences in microstructure and mechanical properties.

4. Carbide Stability in Lithium: An important factor in the lithium corrosion of 2 1/4 Cr - 1 Mo steel is the relative thermodynamic stability of each of the carbides. The free energies of formation of several of the carbides formed in 2 1/4 Cr - 1 Mo steel along with the free energy of formation of lithium carbide are plotted in Figure 3.

According to Figure 3 cementite and Mo_2C are unstable in lithium at 500C. Cementite should react with lithium to form Li_2C_2. This reaction has been directly observed by Beskorovainyi and Ivanov[13,14].

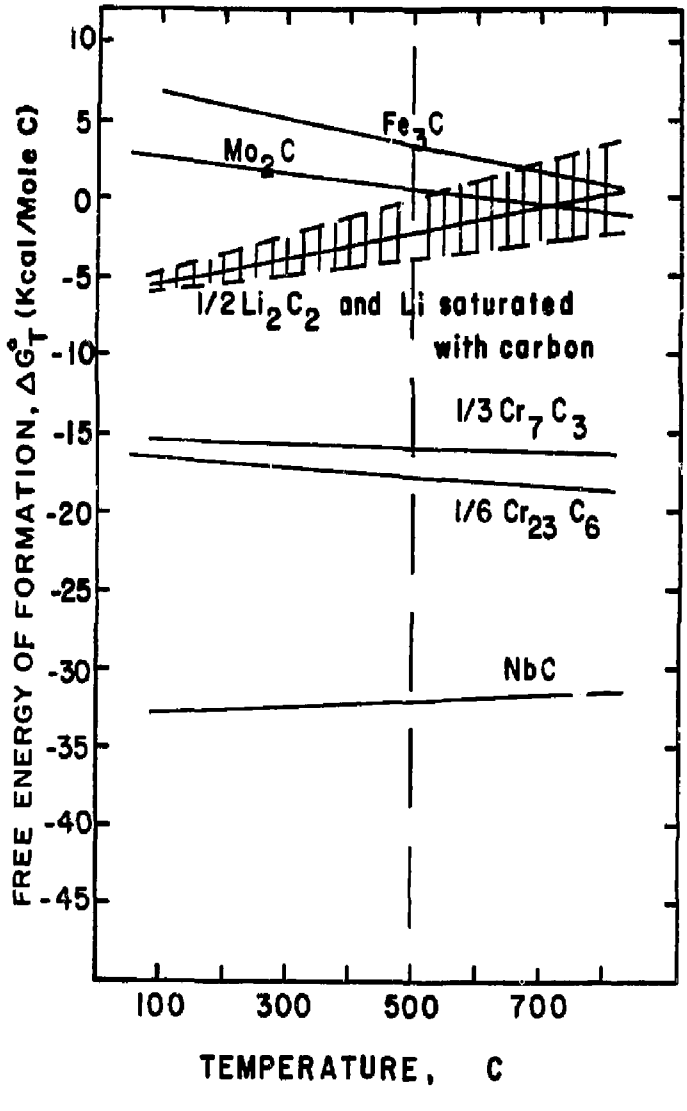

Figure 3. Relative thermodynamic stability of several carbides in carbon saturated lithium.

EXPERIMENTAL PROCEDURE

The chemical compositions of the two alloys used in this investigation are shown in Table I.

TABLE I

Chemical Compositions of the 2 1/4 Cr - 1 Mo Alloys

Alloy	C	Si	Mn	P	S	Cr	Ni	Mo	Nb	Fe
Unstabilized 2-1/4Cr-1Mo	0.12	0.32	0.43	0.018	0.002	2.07	--	1.04	--	bal.
Nb-Stabilized 2-1/4Cr-1Mo	0.09	0.32	0.46	0.012	0.007	2.19	0.55	0.98	1.13	bal.

The metallurgical conditions of weldments of both the unstabilized and niobium-stabilized compositions shown in Table I were varied by post-weld heat treatments representing the minimum and maximum temperatures specified by code. The data matrix for this investigation is shown in Table II. Isothermally transformed and tempered coupons of both unstabilized and unstabilized 2 1/4/Cr - 1 Mo steel were preheated, GTA-welded, then given one of the post-weld heat treatments listed in Table II.

The GTA-welded coupons, along with unwelded coupons for weight loss measurements, were suspended by iron wires in a 2 1/4 Cr - 1 Mo crucible containing molten lithium (with 17.6 w/o lead)

TABLE II

LIQUID LITHIUM CORROSION

OF 2¼ Cr - 1 Mo STEEL WELDMENTS

A. 17.6 w/o Pr in Lithium

B. Heat Treatment: Austenitized (927C) cooled @ 50 c/hr to 704C, isothermally transformed @ 704C (2 hrs), cooled @ 50 c/hr to 500C, furnace cooled, tempered @ 760C for 10 hrs.

C. Pre-Heat: 200C

ALLOY	POST WELD HEAT TREATMENT		
	NONE	10 HRS @ 710C	10 HRS @ 760C
2¼ Cr - 1 Mo Nb-Stabilized	*	*	*
2¼ Cr - 1 Mo Unstabilized	*	*	*

EXPOSURE TIME: 1600 HRS

at 500C. Figure 4 shows a diagram depicting the apparatus used. The crucible was heated by means of an electric resistance furnace, controlled to ± 2C by a thermocouple placed in a well in the crucible. Prior to each test, a thermocouple was briefly immersed in the lithium to determine the actual lithium temperature. Coupons were removed from the lithium at various times and were examined metallographically. The maximum exposure time was 1600 hrs.

All tests were performed in an argon atmosphere glove box. Atmosphere purification equipment maintained the atmosphere at ~100 ppm O_2 and ~400 ppm N_2. This relatively pure atmosphere made it possible to maintain the nitrogen content in the lithium at a very low value (< 100 ppm) when the crucible lid was kept in place. During a test, samples of lithium were periodically removed for nitrogen analysis by means of the Micro-Kjeldahl Technique. Typical measurements of nitrogen content ranged from 45 to 65 ppm, nitrogen levels which approach the limit of detectability for the technique.

To more fully understand the intergranular penetration seen in weld heat affected zones, corrosion tests also were performed on coupons which had been deliberately heat treated to give microstructures susceptible to lithium attack. Coupons of unstabilized 2 1/4 Cr - 1 Mo steel were heat treated so as to produce the coarse-grained bainitic microstructures found in GTA-weld heat affected zones[40]. This was accomplished by quenching specimens from three different austenitizing temperatures (1300C,

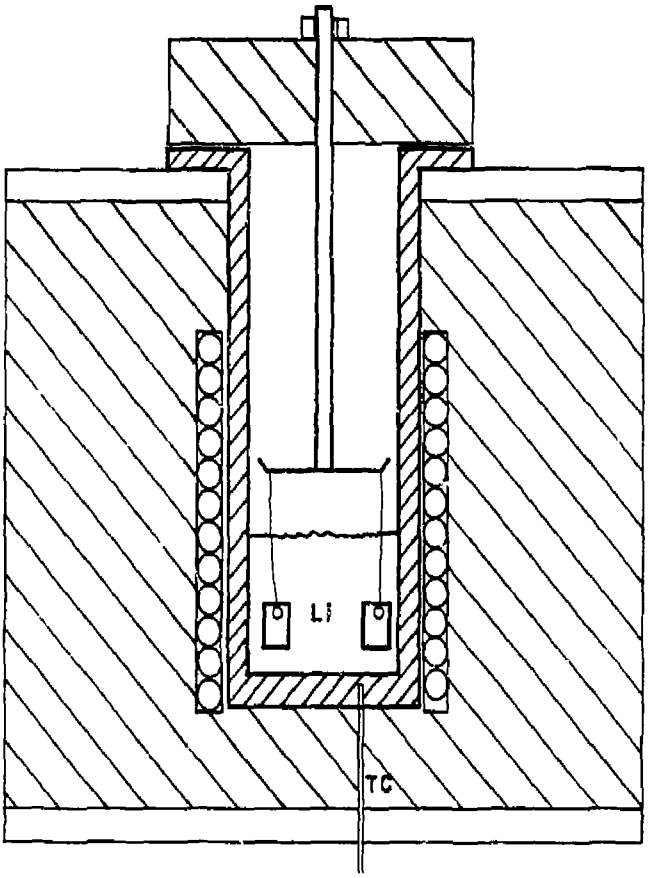

Figure 4: Schematic drawing of apparatus used in weight loss and penetration studies.

1150C, 927C) at three different cooling rates (water quench, oil quench, air cool).

These coupons were exposed to lithium - 17.6 w/o lead in the same manner as the GTA-welded coupons.

RESULTS AND DISCUSSION

Corrosion of GTA Weldments

Figures 5-7 illustrate the effect of microstructure on the relative amount of lithium attack after ~700 hrs. of exposure. Note the severe intergranular attack at prior austenitic grain boundaries in the heat-affected zone of the regular grade weldment with no post-weld heat treatment (Figure 5). The Nb-stabilized material, along with the regular grade weldment in Figure 6 (10 hrs @ 760C post-weld H.T.), seem to be relatively impervious to lithium attack. Figure 8 further illustrates the dramatic improvement in lithium corrosion resistance afforded the weldments of regular grade 2 1/4 Cr - 1 Mo steel by a high temperature post-weld heat treatment. The susceptibility of the various metallurgical conditions to lithium corrosion is summarized graphically in Figure 9. The regular grade material with no post-weld heat treatment experienced the most rapid corrosion, especially during initial stages of attack (< 100 hr exposure). Note (see Figure 9) that a weldment subjected to an 18 ksi tensile stress did not corrode more rapidly than the unstressed weldments.

Weldments of the niobium-stabilized 2 1/4 Cr - 1 Mo steel were quite resistant to corrosion by low nitrogen (~50 ppm) lithium - 17.6 weight percent lead. Only slight penetration (near the limit of measurement) was observed after 1400 hours, and the heat-affected zones of the welds were not preferencially attacked (see Figure 10). Post-weld heat

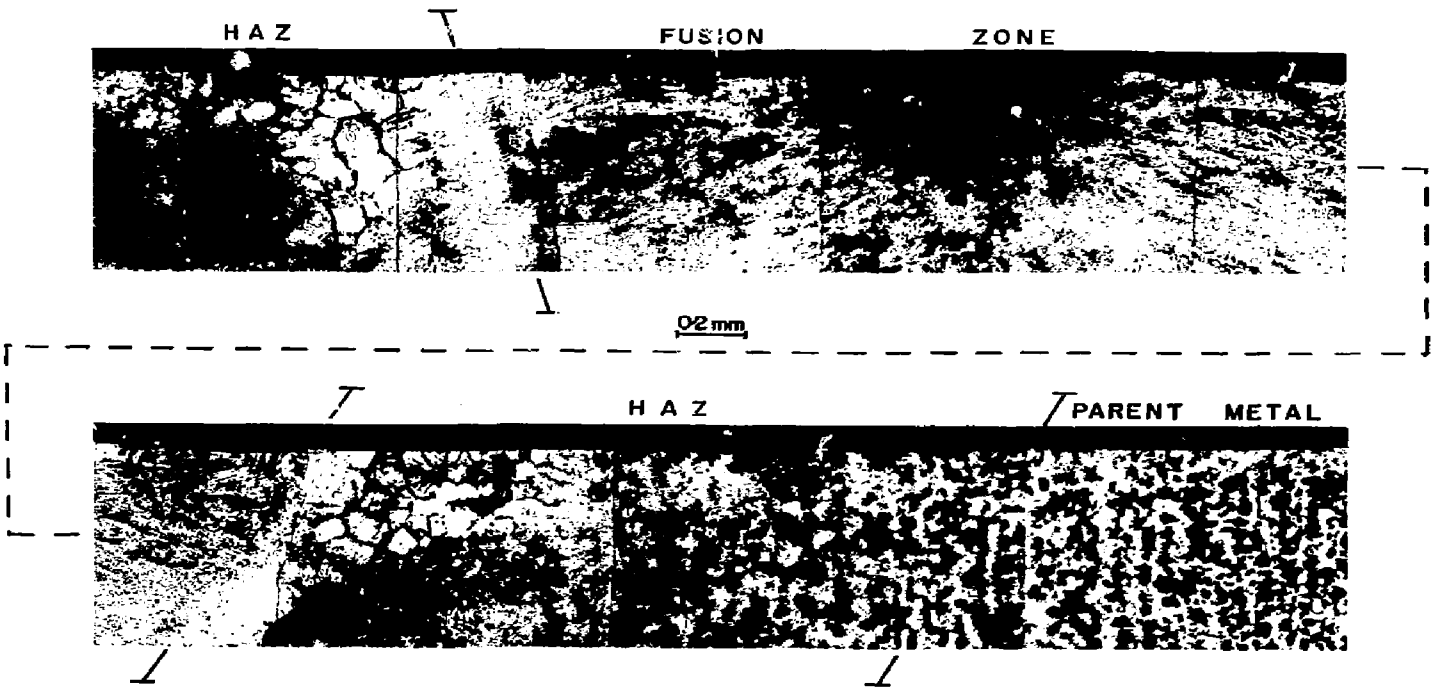

Figure 5: Intergranular penetration of a 2 1/4 Cr-1 Mo (regular grade) GTA weldment at prior austenitic grain boundaries in tne heat affected zone.

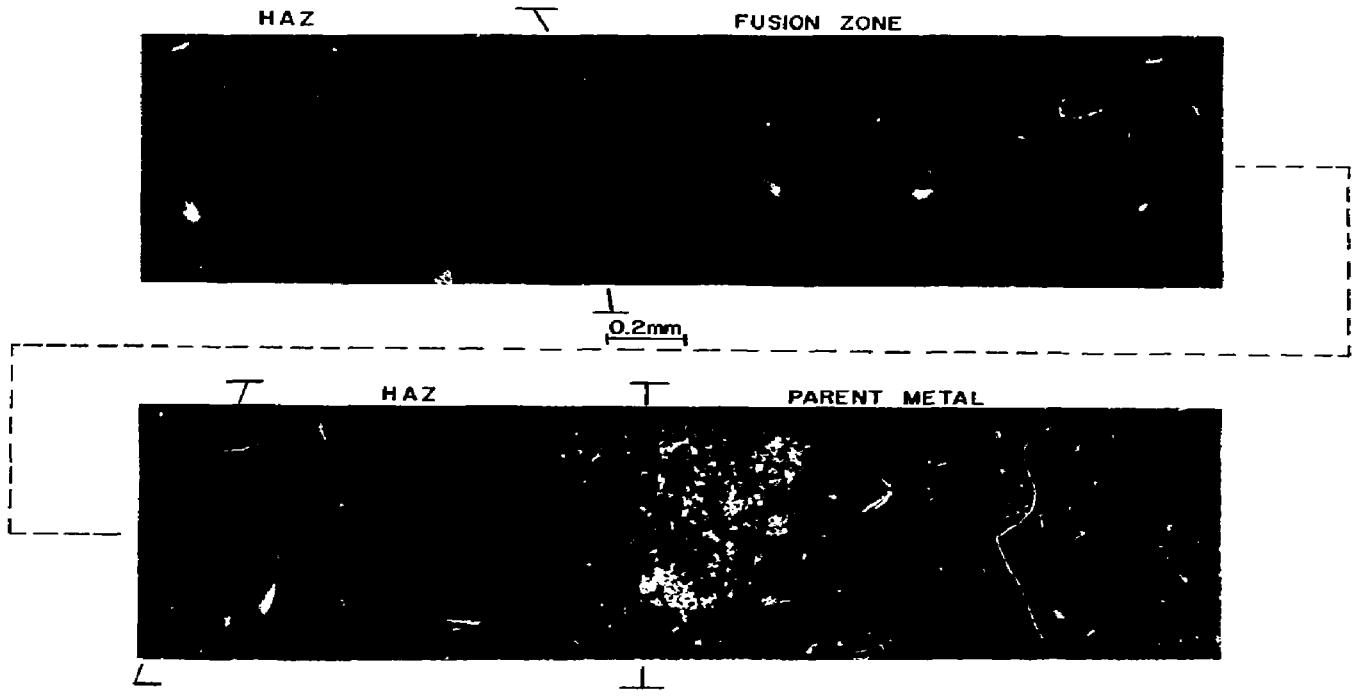

Figure 6: A regular grade 2 1/4 Cr-1 Mo GTA weldments (10 hrs. @ 760C post-weld heat treatment) exposed to lithium-17.6 w/o lead at 500C.

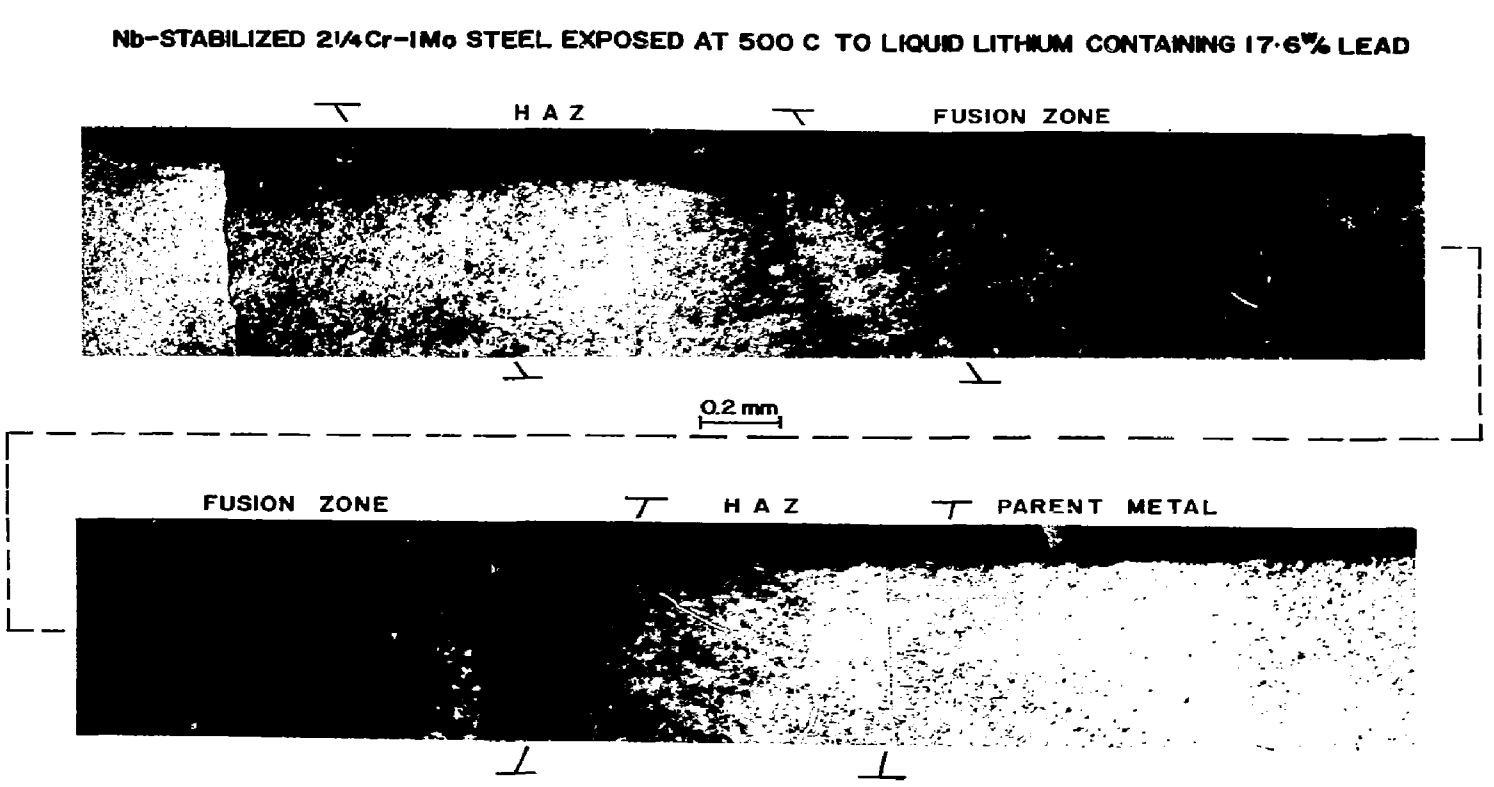

Figure 7: Nb-stabilized 2 1/4 Cr-1 Mo GTA weldments (no post-weld heat treatment) exposed to Li-17.6 w/o Pb at 500C.

Figure 8a: Corrosion of a 2 1/4Cr-1Mo weld HAZ.
No post-weld H.T.
Exposure: 178 hrs in Li-17.6%Pb at 500C.

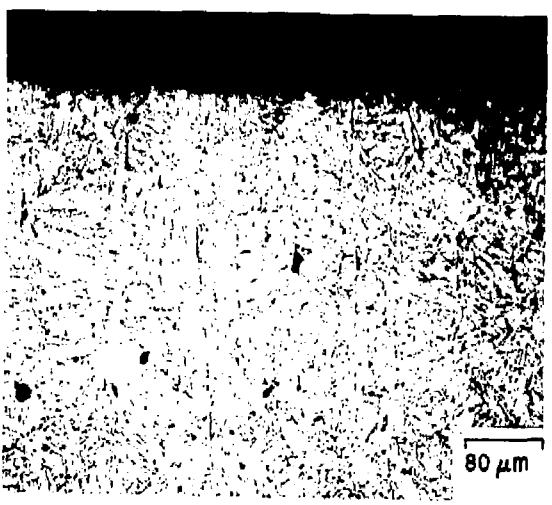

Figure 8b: Corrosion of 2 1/4Cr-1Mo weld HAZ.
Post-weld H.T.: 10 hrs @ 760C.
Exposure: 178 hrs in Li-17.6%Pb at 500C.

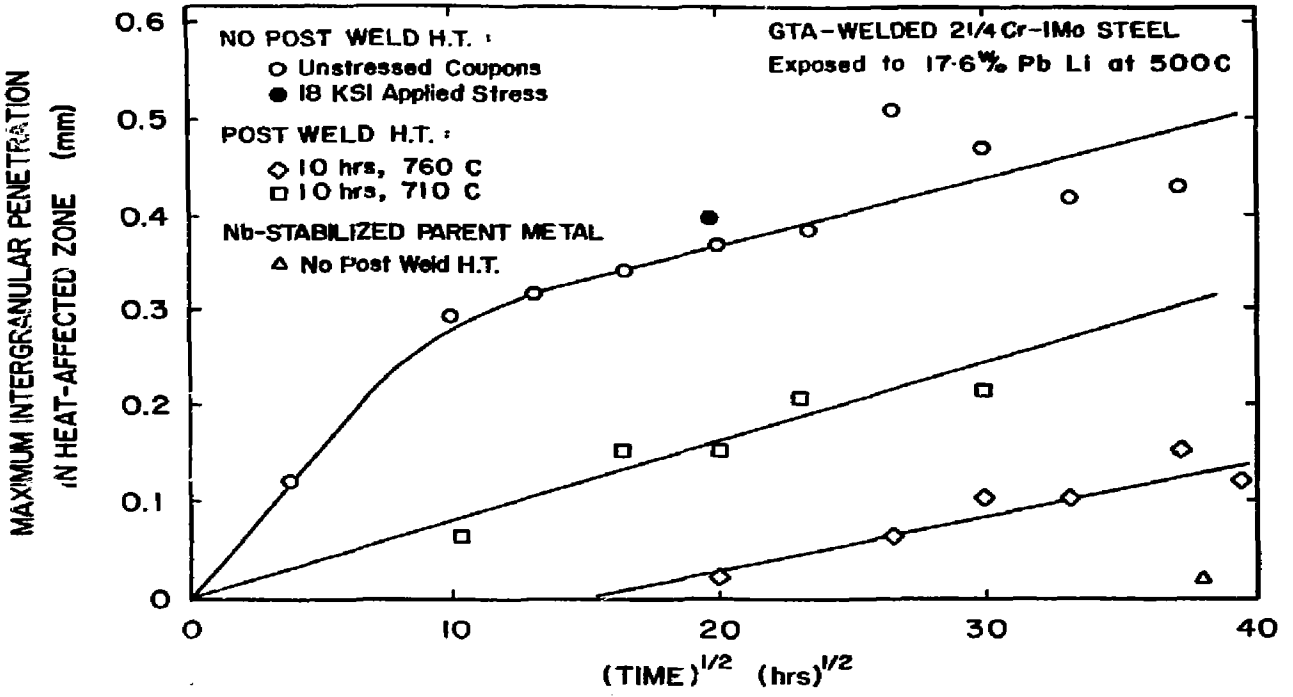

Figure 9: Penetration vs time$^{\frac{1}{2}}$ as a function of post-weld heat treatment and niobium content of GTA weldments exposed to Li-17.6 w/o Pb at 500C.

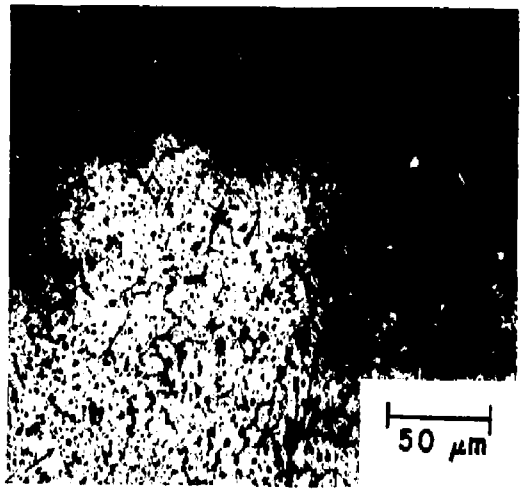

Figure 10: Corrosion of the Nb-stabilized 2 1/4 Cr-1 Mo parent metal. No post-weld H.T. Exposure: 1464 hrs in Li-17.6%Pb at 500C.

treatments did not significantly affect the performance of Nb-stabilized 2 1/4 Cr - 1 Mo steel in lithium - 17.6 weight percent lead.

As was noted previously, post-weld heat treatments dramatically improve the corrosion resistance of regular grade 2 1/4 Cr - 1 Mo steel weldments. The post-weld heat treatments change the appearance of the attack as well as the magnitude. Figure 11 shows the highly localized "worm hole" penetration found in the heat-affected zones of post-weld heat treated specimens (regular grade) exposed to lithium for times up to 1344 hours. The lithium seems to follow second phase particles in the matrix rather than prior austenitic grain boundaries.

The corrosion resistance of a given microstructure of 2 1/4 Cr - 1 Mo steel in lead-lithium can be related to its carbide composition and morphology. Figure 3 indicates that while cementite and Mo_2C are unstable in lithium at 500C, carbides formed during later stages of tempering (such as $Cr_{23}C_6$) are stable in lithium and therefore not susceptible to lithium attack. Since the heat-affected zone of a GTA weldment is subjected to an austenitizing treatment, and a post-weld heat treatment is merely a tempering treatment, the Baker and Nutting[38] study of quenched and tempered 2 1/4 Cr - 1 Mo steel can be utilized to speculate carbides present in the various metallurgical conditions of the weldments. The Baker and Nutting carbide stability diagrams in Figure 2 are repeated in Figure 12 for convenience.

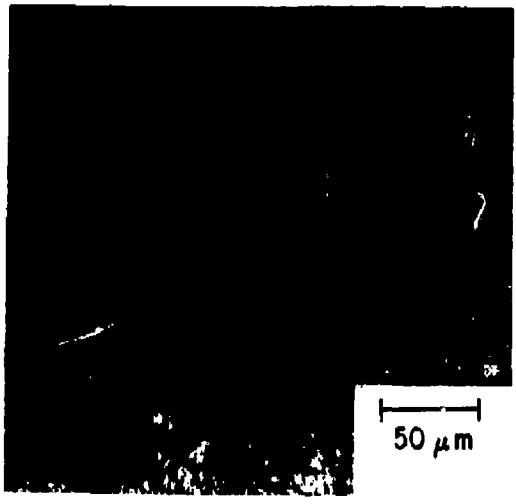

Figure 11a: Corrosion of a 2 1/4 Cr - 1 Mo weld HAZ.
Post-weld H.T: 10 hrs @ 710C.
Exposure: 300 hrs in Li-17.6%Pb at 500C.

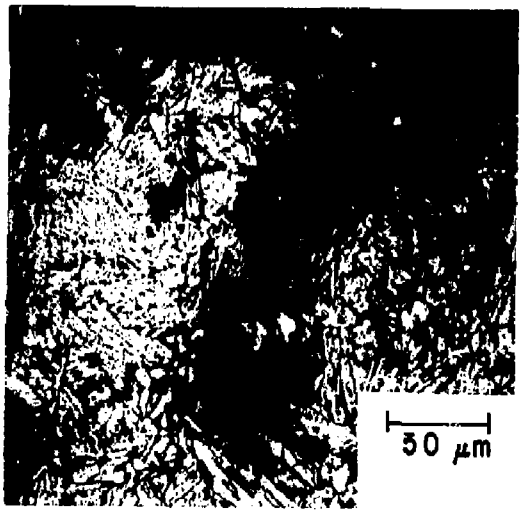

Fig. 11b: Corrosion of a 2 1/4 Cr - 1 Mo weld HAZ.
Post-weld H.T: 10 hrs @ 760C.
Exposure: 1344 hrs in Li-17.6%Pb at 500C.

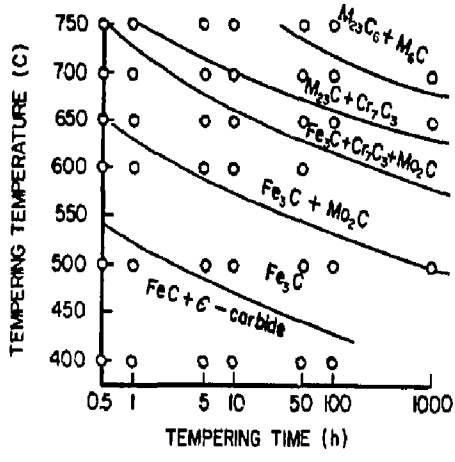

QUENCHED

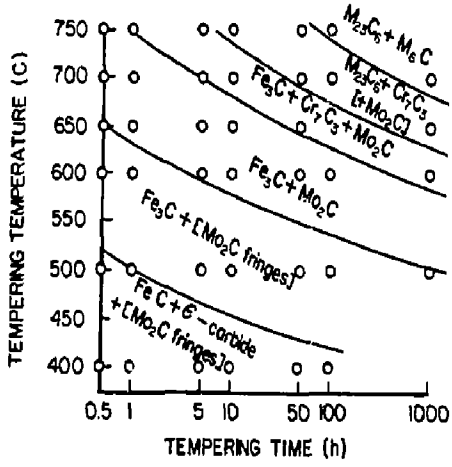

NORMALIZED

Figure 12. Carbide stability diagrams for quenched and tempered and normalized and tempered 2 1/4 Cr - 1 Mo steel.

When 2 1/4 Cr - 1 Mo steel is cooled from an austenitizing temperature, a mixture of cementite and ε-carbide precipitates in a bainitic matrix. We believe that intergranular penetration of the unstabilized GTA-weldments is a result of the dissolution of cementite and/or ε-carbide by the lithium. The ε-carbide is less stable in the bainitic matrix than cementite. Since cementite is thermodynamically unstable in lithium, ε-carbide must also be unstable in lithium. The mechanisms underlying the corrosion of this microstructure are discussed in greater detail in the section of this report which describes the corrosion of simulated weldments.

As was noted previously, the corrosion of coupons with post-weld heat treatments has a different appearance. The attack does not follow prior austenitic grain boundaries as was the case in the untempered heat-affected zones.

According to Figure 12, the post-weld heat treatments should remove nearly all of the Fe_3C from the microstructure. The microstructure should contain primarily stable carbides such as Cr_7C_6 and $M_{23}C_6$. However, Mo_2C, which is unstable at 500C in lithium (see Figure 3), will also be present.

During tempering, Mo_2C "fringes" grow out from carbide-ferrite boundaries. The appearance of the attack in Figure 11 suggests that the lithium penetration follows a path set down by the Mo_2C fringes. Further tempering at sufficiently high temperatures would remove the Mo_2C fringes and increase corrosion resistance. This is evidenced by the greater corrosion resistance of the 760C post-weld heat treatment (see Figure 9).

The niobium-stabilized alloy was extremely resistant to intergranular attack, even when no post-weld heat treatment was applied. This corrosion resistance can be attributed to the formation of stable refractory carbides upon cooling. Since these niobium carbides form rather than cementite, a post-weld heat treatment is not required for good corrosion resistance. The disadvantages of the niobium-stabilized alloy involve weldability, availability and the undesirable nuclear properties of two of the alloying elements, nickel and niobium.

Corrosion of Simulated Weldments

Coupons of regular grade 2 1/4 Cr - 1 Mo steel were heat treated so as to produce the coarse-grained bainitic microstructure found in the corrosion susceptible heat affected zones of GTA weldments. The HAZ microstructure was best approximated by a 1300C austenitizing treatment followed by an oil quench (see Figure 13). These simulated weldments corroded intergranularly, as did the heat-affected zones of actual weldments. Figure 14 shows that significant intergranular attack occurred after only one hour of exposure to the 17.6% Pb-Li liquid at 500C.

The results of corrosion tests on specimens representing all the weld-simulating heat treatments are summarized in Figure 15. The penetration vs time$^{1/2}$ curve for the GTA-welded coupons is superimposed for comparison. Note the increase in penetration rate caused by an increase in austenitizing temperature, and the

HEAT-AFFECTED ZONE
GTA-WELDED 2¼Cr-1Mo STEEL

25 μm

WELD-SIMULATING HEAT TREATMENT
(AUSTENITIZED AT 1300 C, OIL-QUENCHED)

Figure 13: Comparison of microstructure from the heat affected zone of an actual FTA weldments and from a specimen heat treated (oil-quenched from 1300C) to simulate the weldment's heat affected zone.

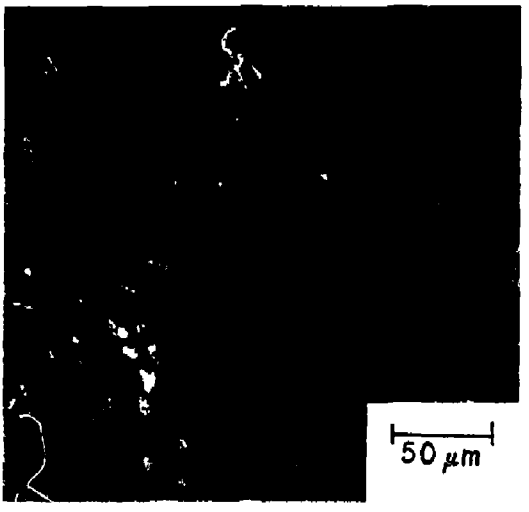

Figure 14: Intergranular penetration of a simulated HAZ (oil quenched from 1300C) specimen. Exposure: 1 hr in Li-17.6%Pb at 500C.

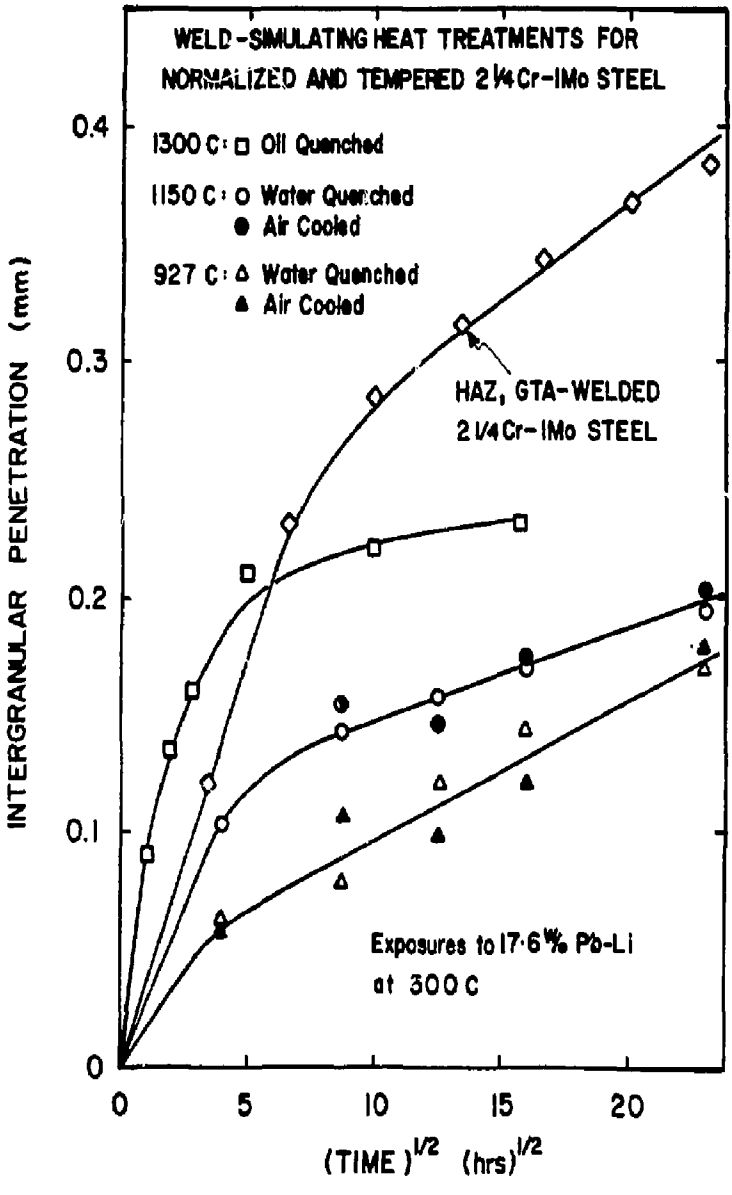

Figure 15. Intergranular penetration of 2 1/4 Cr - 1 Mo steel at 500C in lithium - 17.6 w/o lead as a function of time and heat treatment compared to the penetration of a GTA weldment of HAZ.

insensitivity of the penetration rate to the cooling rate from the austenite range.

An obvious feature of Figure 15 is a change in slope in the penetration vs time$^{1/2}$ curves at approximately 25 hours. This change probably corresponds to a change in mechanism or rate controlling step. A possible explanation for the slope change is that it is associated with a carbide reaction within the steel. When 2 1/4 Cr - 1 Mo steel is cooled rapidly from the austenitic range, it transforms bainitically to a microstructure comprised of cementite and ε-carbide precipitates in a ferrite matrix. Upon tempering at 500C, the less stable ε-carbide is replaced by cementite and eventually Mo_2C (see Figure 12). According to Figure 12, the time required to replace ε-carbide by tempering 2 1/4 Cr - 1 Mo steel at 500C is approximately the time at which the penetration curves in Figure 15 change slope. Since cementite is readily attacked by lithium at 500C, and ε-carbide is unstable relative to cementite in this steel at 500C, one would expect even more rapid lithium attack of any ε-carbide present. A rapid penetration by lithium would result until ε-carbide had been converted to cementite; then penetration would continue at a rate determined by the interaction of cementite with lithium.

Auger Spectroscopy

A GTA-welded coupon of 2 1/4 Cr - 1 Mo steel exposed to lithium (no lead) for 240 hours at 500C was fractured in a 10^{-9} Torr vacuum. The sample was fractured in the heat-affect zone

where intergranular attack had occurred, and the fracture surface was analyzed by Auger spectroscopy.

Figure 16 shows the Auger spectra from three regions on the fracture surface. A high concentration of sulfur and oxygen was found at the prior austenitic grain boundaries, even in grain boundaries not yet reached by the lithium. Apparently, the sulfur segregation to the grain boundaries is a result of the temperature gradients imposed by the welding process. It is not known what role, if any, the sulfur and oxygen play in the corrosion of this steel by lithium.

Weight Loss

The weight loss of both regular grade and Nb-stabilized 2 1/4 Cr - 1 Mo steel in low nitrogen (~50 ppm) lithium - 17.6 weight percent lead was negligible (< 0.2 mg/cm^2 after 1600 hours exposure). It was nearly impossible to collect meaningful data from these tests because the measured values of weight loss were of the same order of magnitude as the maximum sensitivity of the analytical balance.

Data collected during the first contract year showed that measurable weight loss of 2 1/4 Cr - 1 Mo steel occurred in lithium containing ~500 ppm nitrogen. The rate of dissolution was accelerated when the nitrogen content increased to ~2500 ppm.

Apparently weight loss will not be a significant problem in lithium loops, as long as the nitrogen level is maintained at a low value (< 100 ppm). However, these tests were performed in static lithium. It remains to be seen what effect the velocity of lithium will have on the dissolution rate of the steel.

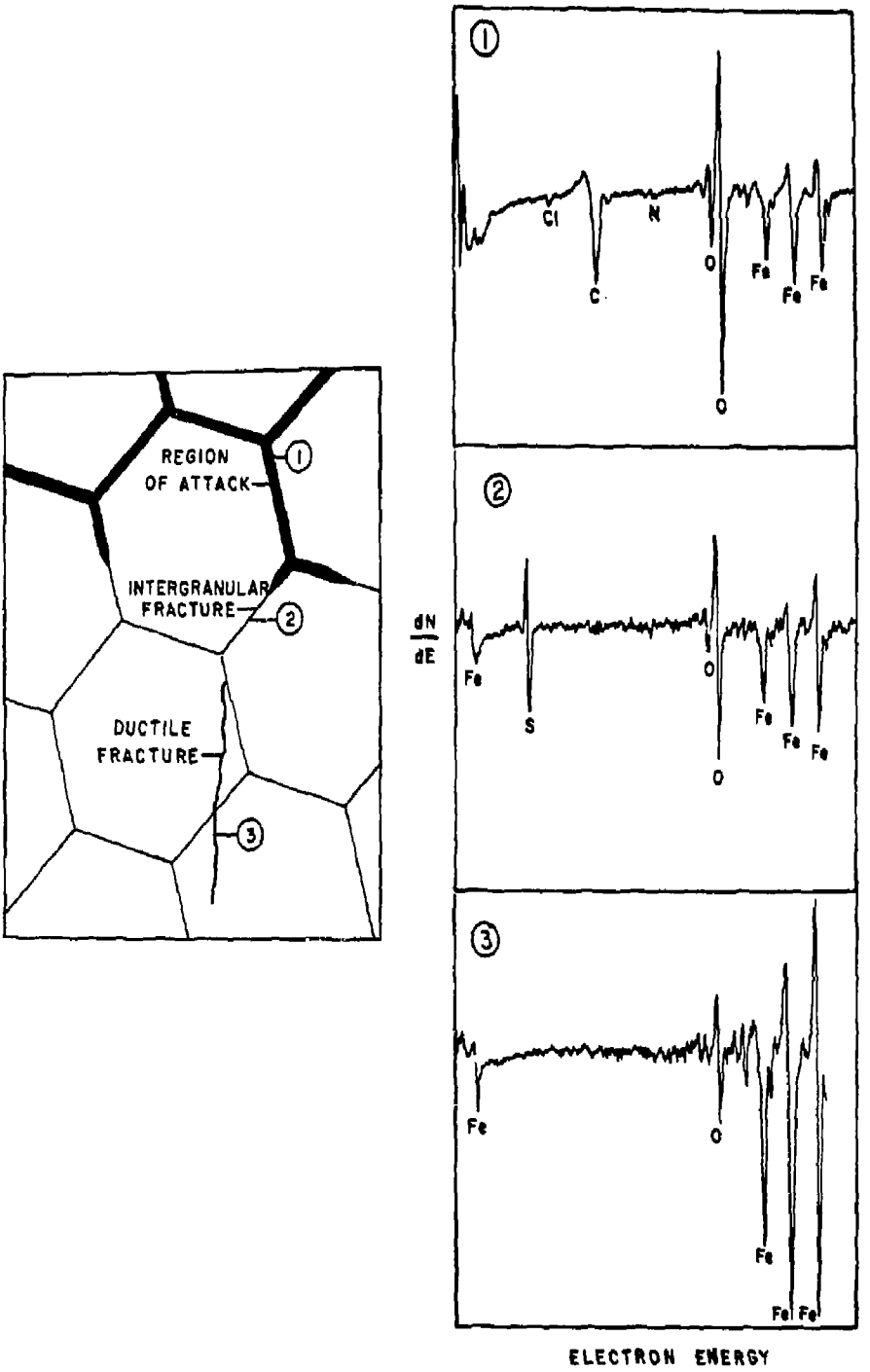

Figure 16. Auger spectra of three regions of a GTA weldment fractured along a corroded grain boundary. The specimen was exposed to lithium (no lead) at 500C for 240 hrs.

CONCLUSIONS AND RECOMMENDATIONS

Niobium stabilized 2 1/4 Cr - 1 Mo steel exhibits the best lithium corrosion resistance of all candidate alloys tested to date. However, the problems of cost, availability, and weldability, as well as the nuclear problems associated with this alloy are sufficient reasons to justify a concentrated effort to improve the lithium corrosion resistance of the regular grade of 2 1/4 Cr - 1 Mo steel.

The lithium corrosion resistance of the regular grade of 2 1/4 Cr - 1 Mo steel can be vastly improved with a proper post-weld heat treatment, but even greater improvements are needed if the steel is to meet conventional corrosion design criteria. Study to date indicates that if weldments were tempered sufficiently long at 760C to remove all Mo_2C from the microstructure, even greater resistance to attack by low nitrogen lithium could be achieved. Corrosion tests should eventually be performed on regular grade 2 1/4 Cr - 1 Mo steel weldments which have been given a long-term (> 25 hrs) post-weld temper at 760C. Improvement in lithium corrosion resistance of regular grade 2 1/4 Cr - 1 Mo steel may also be achieved by employing a quench and temper heat treatment as opposed to an isothermal anneal. Quenched microstructures have a significantly more homogenous distribution of carbides than isothermally annealed microstructures, and if properly tempered, should provide excellent lithium corrosion resistance. Furthermore, the toughness of such a lower bainite microstructure should be

significantly better than that of the ferrite-bainitic microstructure created by an isothermal anneal.

Numerous parameters, all potentially deleterious to the lithium corrosion resistance of 2 1/4 Cr - 1 Mo steel, remain to be investigated. Two such variables are velocity effects and lead content in the lithium. It is recommended that the Colorado School of Mines devote the 1980 contract year to systematic screening tests evaluating the effects of velocity and lead content on the lithium corrosion susceptibility of 2 1/4 Cr - 1 Mo steel.

ACKNOWLEDGEMENTS

The support of the Basic Sciences Division, Department of Energy, and the National Association of Corrosion Engineers for the research funding supplementary to this contract is gratefully acknowledged. The assistance of Dr. J.B. Lumsden, Rockwell International, in performing the auger spectroscopy was very helpful, and the continued interest and support of Dr. Nate Hoffmann has been invaluable. Considerable assistance from our colleagues in reactive metals research, Drs. David Olson and David Matlock, was gratefully received.

REFERENCES

1. Hoffman, E. E., Corrosion of Materials by Lithium at Elevated Temperatures, ORNL 2924, (1960).

2. Wilkinson, W.D. and Yagee, F.L., Attack on Metals by Lithium, ANL 4990, (1950).

3. Cunninghan, J.E., Resistance of Metallic Materials in Corrosive Attack by High-Temperature Lithium, ORNL-CF-51-7-135, (1951).

4. Brasunas, A., Interim Report on Static Liquid-Metal Corrosion, ORNL 1647, (1954).

5. Olson, D.L. and Bradley, W.L., The Corrosion of Ferrous Alloys in Nitrogen-Contaminated Liquid Lithium, ERDA Conference Report CONF-760503-P1, pp. 446-452, (1976).

6. Bates, D.A., Edwards, G.R. and Olson, D.L., "An Evaluation of Engineering Alloys for High Temperature Lithium Containment," Materials Performance, 19, pp. 40-48.

7. Hoffman, E.E. and Manly, W.D., Advances in Chemistry, Am. Chem. Soc., Series 19, pp. 82-92, (1957).

8. Manly, W.D., Corrosion, 12, p. 336, (1956).

9. Weeks, J.R. and Klamut, C.J., Liquid-Metal Corrosion Mechanisms, Corrosion of Reactor Materials I, International Atomic Energy Agency, Vienna, (1962).

10. Popovich, V., Goikham, M.S., Datishin, A.M., Toropovskaya, I.N., Shtykalo, I.G., and Chaevskii, M.I., Fiz. Khim. Mikh. Mat., 3, pp. 24-32, (1967).

11. Jordan, W., Bradley, W.L., and Olson, D.L., Nucl. Tech., 29, pp. 209-214, (1976).

12. Whipple, T.A., Olson, D.L., Bradley, W.L., and Matlock, D.K., Nucl. Tech., 39, pp. 75-83, (1978).

13. Beskorovainyi, N.M., Ivanov, V.K., and Zuev, M.T., Behavior of C in Systems of the Metal-Molten Metal-C Type, High Purity Metals and Alloys-Fabrication, Properties and Testing No. 5 Atomizdat, Moscow, 1966, Eng. Translation by Consultants Bureau, p. 107, (1967).

14. Beskorovainyi, N.M. and Ivanov, V.K., High Purity Metals/Alloys Fabrication, Properties and Testing, pp. 121-129.

15. Selle, J.E., Corrosion of Iron Base Alloys by Lithium, Proceedings of International Conference on Liquid Metal Technology in Energy Production, Champion, PA, May 3-6, 1976, Report CONF-760503-P2, pp. 455-461, (1976).

16. Devan, J.H., Selle, J.E., and Morris, A.E., Review of Lithium Iron-Base Alloy Corrosion Studies, ORNL/TM 4927, (1976).

17. Steinmeyer, P., Colorado School of Mines, private communication, (1978).

18. Bunker, C.E., Test Results of Li Mass Transfer Loop LDL-1, Report TIM-405, (1957).

19. Seebold, R.E., Corrosion, 16, p. 468, (1960).

20. Boyer, M.H., Information of the Resistance of Materials to Attack by Molten Lithium, Report CRD-T2C-33, (1951).

21. Kolodney, M. and Minushkin, B., A Method for Determining the Solution Rate of Container Metals in Lithium, Report NDA-41, (1951).

22. Gorkham, M.S. and Chaevskii, M.I., Fiz. Khim. Mekh. Mat., 6, pp. 106-108, (1970).

23. Reser, G.N., Predicting the Controlling Mode in the Corrosion of 304L Stainless Steel by Liquid Lithium, M.S. Thesis, Colorado School of Mines, T-2019, (1977).

24. Schlager, R.J., Olson, D.L., and Bradley, W.L., Nucl. Tech., 27, pp. 439-441, (1975).

25. Patterson, R.A., Schlager, R.J., and Olson, D.L., J. Nuc. Mat., 57, pp. 312-316, (1975).

26. Dana, A.W., Baker, O.H., Fergeson, M., Investigation of Metal Transport by Liquid Lithium, Tech. Rept. V, B & W-5320, DC-52-27-45, (1952).

27. Elrod, H.G., Fouse, R.R., and Richards, P.B., Erosion and Heat Transfer with Molten Lithium, Final Report, Rept. NEPA 1837, B & W Rept. 5217, (1951).

28. Dmukhovskaya, I.G., Shatinskii, V.F., and Sinelnikova, O.G., Zaschita Metallov, 11, pp. 21-26, (1975).

29. Goikhman, M.S., Fiz. Khim. Mekh. Mat., 6, pp. 107-109, (1970).

30. Leavenworth, H.W. and Cleary, R.E., Acta Met., 9, p. 519, (1961).

31. Katsuta, H. and Furukawa, J., J. of Nuc. Met., 71, pp. 95-104, (1977).

32. DeMastry, J.A., Nuc. Appl., 3, pp. 127-134, (1967).

33. Kleuh, R.L., Met. Trans., 5, pp. 875-879, (1974).

34. Brehm, W.F., Gregg, J.L., Che Yu Li, Trans. AIME, 242, pp. 1205-1210.

35. Lautzenheiser, C.E., Use of Quenched and Tempered 2 1/4 Cr - 1 Mo Steel, Climax Molybdenum Co., New York, May 1965.

36. Habrahen, L.J. and Economopoulos, M., Transformations and Hardenability in Steels Symposium, Climax Molybdenum Co. and the University of Michigan, 1967, p. 71.

37. Copeland, J.F. and Pense, A.W., Hardenability: Key to Vessel Plate Strength, Hydrocarbon Processing, April 1974.

38. Baker, R.G. and Nutting, J., The Tempering of 2 1/4 Cr - 1 Mo Steel After Quenching and Normalizing, J. Iron and Steel Inst., 192, No. 7, (1959), p. 257.

39. Leitnaker, J.M., Kluehn, R.L., and Lang, W.R., Met. Trans., 6A, p. 1949, (1975).

40. Alberry, P.J. and Jones, W.K.C., Metals Technology, pp. 360-364, (1977).